

Controllable continuous evolution of electronic states in a single quantum ringTapash Chakraborty,^{1,*} Aram Manaselyan,^{2,†} Manuk Barseghyan,^{2,‡} and David Laroze^{3,4,§}¹*Department of Physics and Astronomy, University of Manitoba, Winnipeg, Canada R3T 2N2*²*Department of Solid State Physics, Yerevan State University, 0025 Yerevan, Armenia*³*Instituto de Alta Investigación, CEDENNA, Universidad de Tarapacá, Casilla 7D Arica, Chile*⁴*Yachay Tech University, School of Physical Sciences and Nanotechnology, 00119-Urcuquí, Ecuador*

(Received 17 July 2017; revised manuscript received 17 September 2017; published 31 January 2018)

An intense terahertz laser field is shown to have a profound effect on the electronic and optical properties of quantum rings where the isotropic and anisotropic quantum rings can now be treated on equal footing. We have demonstrated that in isotropic quantum rings the laser field creates unusual Aharonov-Bohm oscillations that are usually expected in anisotropic rings. Furthermore, we have shown that intense laser fields can restore the *isotropic* physical properties in anisotropic quantum rings. In principle, all types of anisotropies (structural, effective masses, defects, etc.) can evolve as in isotropic rings in our present approach. Most importantly, we have found a continuous evolution of the energy spectra and intraband optical characteristics of structurally anisotropic quantum rings to those of isotropic rings in a controlled manner with the help of a laser field.

DOI: [10.1103/PhysRevB.97.041304](https://doi.org/10.1103/PhysRevB.97.041304)

Research on the electronic and optical properties of quantum confined nanoscale structures, such as quantum dots and quantum rings, has made great strides in recent years in unraveling new phenomena and their enormous potentials in device applications. In this context, quantum rings with their doubly connected structures attract special attention. Their unique topological structures provide a rich variety of fascinating physical phenomena in this system. Observation of the Aharonov-Bohm (AB) oscillations [1] and the persistent current [2] in small semiconductor quantum rings (QRs) and recent experimental realization of QRs with only a few electrons [3,4] have made QRs an attractive topic of experimental and theoretical studies for various quantum effects in these quasi-one-dimensional systems [5]. In particular, recent work has indicated the great potentials of QRs as basis elements for a broad spectrum of applications, starting with terahertz detectors [6], efficient solar cells [7], and memory devices [8] through electrically tunable optical valves and single-photon emitters [9,10]. We have also worked previously on QRs in new materials, such as graphene systems [11] and ZnO [12] with interesting outcomes reported in Refs [13,14], respectively.

Although almost circular or slightly oval-shaped QRs have been fabricated by various experimental groups [15–18], anisotropic QRs are the ones most commonly obtained during the growth process [17,19–21]. Theoretically the effect of anisotropy on electronic, magnetic, and optical properties of quantum rings have been investigated by various authors [22–29]. In those studies, different types of anisotropies were explored. For example, in Refs. [22,23,27,28] the shape anisotropy of the QR was considered, whereas in Refs. [24–26] the anisotropy associated with defects was studied, and in

Ref. [29] the effective-mass anisotropy was investigated. In all these cases it was shown that the anisotropy can dramatically alter the AB oscillations in the QR. In particular, in Ref. [29] it was demonstrated that the unusual AB oscillations caused by the effective-mass anisotropy in the QR can be converted to usual AB oscillations if the QR has an elliptical shape. However, in order to experimentally confirm these results, one needs to grow QRs with different anisotropies and compare their measurable optical and magnetic characteristics individually.

Here we consider the effect of a terahertz intense laser field (ILF) on isotropic and anisotropic QRs and demonstrate that in the case of isotropic QRs the ILF can create unusual AB oscillations that are characteristics of anisotropic rings. Additionally, we have shown that in the case of anisotropic QRs the ILF can be used as an anisotropy controlling tool with the help of which it will be possible to visualize both the isotropic and the anisotropic properties on a single QR. For example, we have shown that the unusual AB oscillations obtained for the elliptic QR can be made usual with the help of the ILF. Therefore the ILF can unify all the electronic properties of isotropic and anisotropic rings in a single system.

Our system consists of a two-dimensional anisotropic QR structure containing electrons that are under the action of laser radiation and an external magnetic field that is oriented along the growth direction. The laser field is represented by a monochromatic plane wave of frequency ω . The laser beam is nonresonant with the semiconductor structure and linearly polarized along a radial direction of the structure (chosen along the x axis). In the noninteracting case, the electron motion is described by the solution of the time-dependent Schrödinger equation,

$$\left[\frac{1}{2m} \left(\hat{\mathbf{p}} - \frac{e}{c} [\mathbf{A}(t) + \mathbf{A}_m] \right)^2 + V(x, y) \right] \Phi(x, y, t) = i\hbar \frac{\partial}{\partial t} \Phi(x, y, t), \quad (1)$$

*Tapash.Chakraborty@umanitoba.ca

†amanasel@ysu.am

‡mbarsegh@ysu.am

§dlarozen@uta.cl

where m is the electron effective mass, \mathbf{p} is the lateral momentum of the electron, e is the absolute value of the electron charge, $\mathbf{A}(t) = \mathbf{e}_x A_0 \cos(\omega t)$ is the laser-field's vector potential, where \mathbf{e}_x denotes the unit vector on the x axis. In Eq. (1), \mathbf{A}_m is the vector potential of the magnetic field which is chosen to be $\mathbf{A}_m = (0, Bx, 0)$. In this case the scalar product is $[\mathbf{A}(t) \cdot \mathbf{A}_m] = 0$.

For the lateral confinement potential $V(x, y)$ we have chosen the model of a finite square-well type, which can be written as

$$V(x, y) = \begin{cases} 0, & \text{if } R_1 \leq \sqrt{x^2 + (y/\sqrt{1 - \varepsilon^2})^2} \leq R_2, \\ V_0, & \text{otherwise,} \end{cases} \quad (2)$$

where R_1 and R_2 are the inner and outer radii, respectively, of the QR and ε describes the anisotropy of the QR ($\varepsilon = 0$ corresponds to the case of the circular QR) [29].

Using the dipole approximation and the Kramers-Henneberger unitary transformation [30] in the high-frequency regime [31–38] the laser-dressed energies of the QR can be obtained from the following time-independent Schrödinger equation [39]:

$$\left[\frac{1}{2m} \left(\hat{\mathbf{p}} - \frac{e}{c} \mathbf{A}_m \right)^2 + V_d(x, y) \right] \Phi_d(x, y) = E_d \Phi_d(x, y), \quad (3)$$

where $V_d(x, y)$ is the time-averaged laser-dressed potential that can be expressed by the following analytical expression [40,41]:

$$V_d(x, y) = \frac{V_0}{\pi} \text{Re} \left[\pi - \theta(\alpha_0 - x - \Gamma_1) \arccos \left(\frac{\Gamma_1 + x}{\alpha_0} \right) + \theta(\alpha_0 - x - \Gamma_2) \arccos \left(\frac{\Gamma_2 + x}{\alpha_0} \right) - \theta(\alpha_0 + x - \Gamma_1) \arccos \left(\frac{\Gamma_1 - x}{\alpha_0} \right) + \theta(\alpha_0 + x - \Gamma_2) \arccos \left(\frac{\Gamma_2 - x}{\alpha_0} \right) \right], \quad (4)$$

where $\theta(u)$ is the Heaviside unit-step function and $\Gamma_i = \text{Re}[\sqrt{R_i^2 - (y/\sqrt{1 - \varepsilon^2})^2}]$. It is worth mentioning that, in the case of the more realistic confinement potential other than the square-well type, the laser-dressed potential cannot be presented by the analytical form and the obtained results do not change qualitatively. The parameter $\alpha_0 = (e/m\epsilon_h^{1/4}v^2)\sqrt{I/(2c\pi^3)}$ describes the strength of the laser field and comprises both the intensity I and the frequency ν of the laser field that can be chosen for a broad range in units of KW/cm^2 and terahertz correspondingly [35]. ϵ_h is the high-frequency dielectric constant of the system. In Fig. 1 the schematic of the dressed potential for different values of the ILF parameter α_0 is presented. The circular and elliptic cases of QRs are shown. The laser-dressed energy eigenvalues E_d and eigenfunctions $\Phi_d(x, y)$ may be obtained by solving Eq. (3) with the help of the exact diagonalization technique. The eigenfunctions are presented as a linear expansion of the eigenfunctions of the two-dimensional rectangular infinitely high potential well [40,41]. In our calculations we have used 361 basis states which are adequate for determining the first few energy eigenvalues with high accuracy.

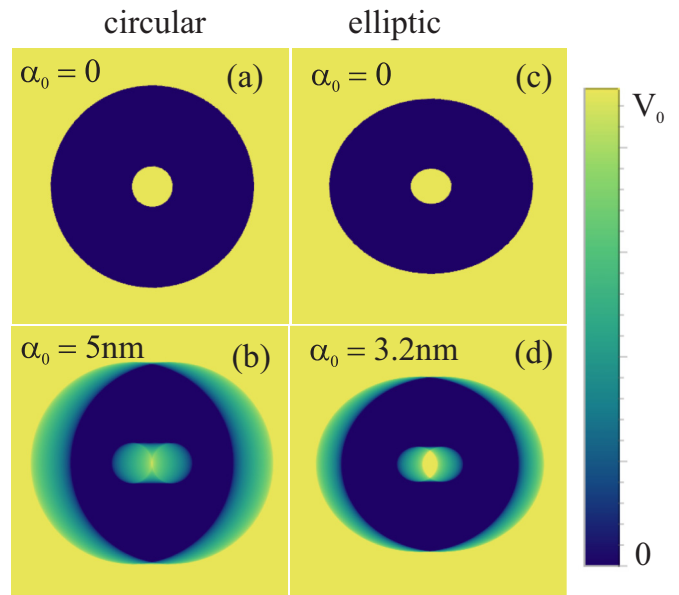


FIG. 1. The density plot of the dressed confinement potential for different values of the ILF parameter α_0 for both circular and elliptic QRs.

We have also considered here the intraband optical transitions in the conduction band. According to the Fermi golden rule for the x polarization of the incident light the intensity of absorption in the dipole approximation is proportional to the square of the matrix element $M_{fi} = \langle f|x|i \rangle$ when the transition goes from the initial-state $|i \rangle$ to the final-state $|f \rangle$.

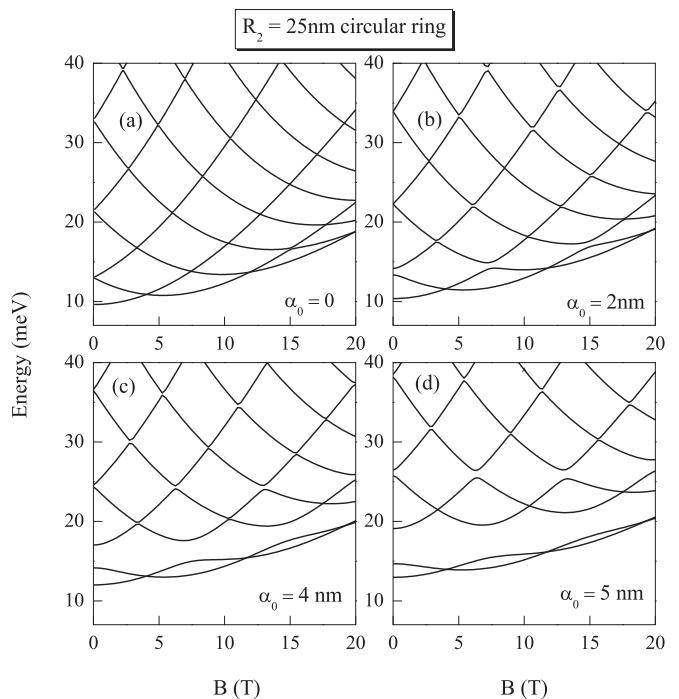


FIG. 2. The low-lying energy levels of a circular QR as a function of the magnetic-field B for different values of the laser-field parameter α_0 . The results are for $R_2 = 25$ nm.

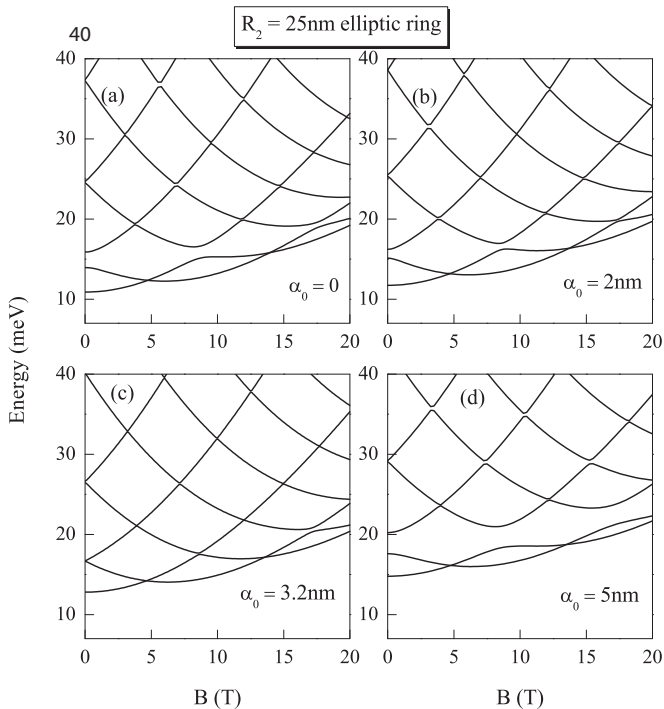


FIG. 3. The low-lying energy levels of an elliptic QR as a function of the magnetic-field B for different values of α_0 . The results are for $R_2 = 25$ nm.

In this Rapid Communication we always consider $|i\rangle$ to be the ground state.

Our numerical studies are carried out for GaAs QRs having parameters $V_0 = 228$ meV, $m = 0.067m_0$ (m_0 is the free-

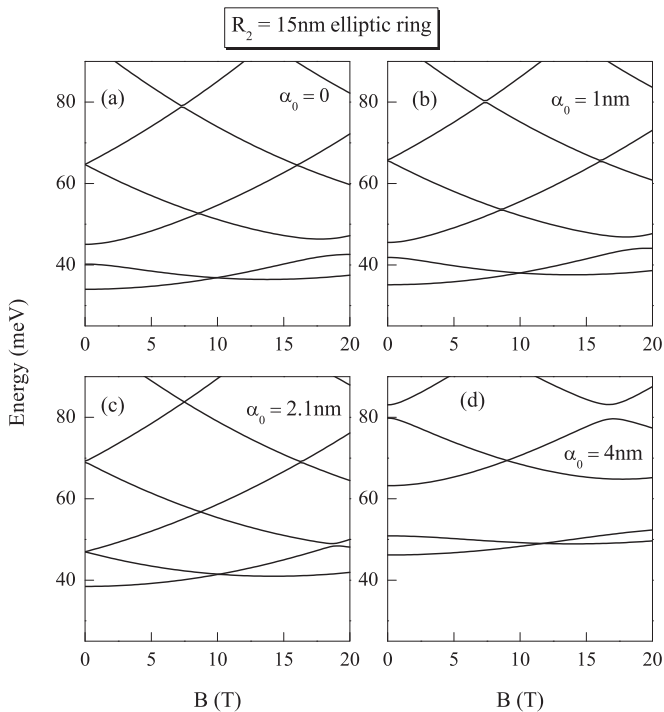


FIG. 4. The low-lying energy levels of an elliptic QR as a function of the magnetic-field B for different values of α_0 . The results are for $R_2 = 15$ nm.

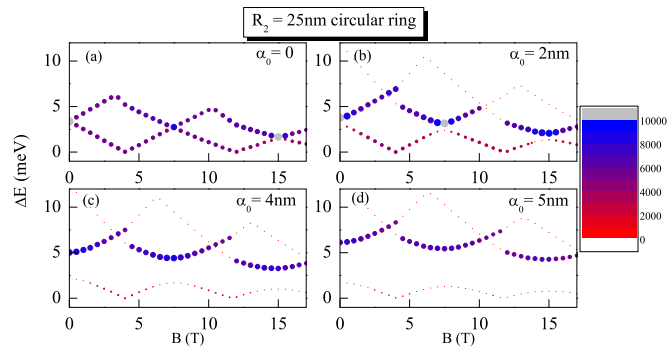


FIG. 5. Dipole-allowed optical transition energies as a function of magnetic-field B for different values of α_0 . The results are for a $R_2 = 25$ -nm circular QR. The size and the color of the circles are proportional to the intensity of the calculated optical transitions.

electron mass), $\epsilon_h = 10.5$, $R_1 = 5$ nm [42]. In Fig. 2, the low-lying energy levels of the circular QR with an outer radius of $R_2 = 25$ nm are presented as a function of the magnetic-field B for various values of the laser-field parameter α_0 . In Fig. 2(a) the usual AB effect has been observed without the laser field, which corresponds to the case of a circular QR. The ILF applied on a QR creates an anisotropy in the confinement potential [Fig. 1(b)] as a result of which the effective length of the confinement along the x direction decreases in the lower part of the QR potential well. It is worth noting that, with the increase in α_0 , the anisotropy of the QR is strengthened and the degeneracy of the excited states at $B = 0$ disappears. With an increase in α_0 due to the reducing symmetry from C_∞ to C_2 , one should expect an energy spectrum split into noncrossing pairs of states which in turn cross repeatedly as B increases (each pair of repeatedly crossing states containing one instance of each of two C_2 symmetries). A similar behavior of the energy levels, which can be called “unusual” AB oscillations, was reported earlier in QRs by other authors that is caused by the effective-mass anisotropy [27,29] and structural distortions in QRs [23]. For $\alpha_0 = 2$ nm, only the ground and first excited states feel the deformation of the potential [see Fig. 2(b)]. Whereas, for larger values of α_0 more excited states start to feel the deformation of the QR confinement potential, and the two periodically crossing pairs can be visible [Fig. 2(d)].

Let us now consider the case of the anisotropic QR under the action of the ILF. From Eq. (2) and Fig. 1(c) it is clear that if $\epsilon \neq 0$ the undressed confinement potential is anisotropic and the QR is compressed along the y direction. On the other hand the laser field brings an anisotropy of the confinement potential along the x direction due to which the bottom of the effective confinement potential can have an almost circular form [see Figs. 1(c) and 1(d)]. Therefore, we have two competing different effects, the first one is caused by the structural anisotropy of the system, whereas the other is caused by the external ILF. In Fig. 3 the magnetic-field dependence of the low-lying energy levels is presented for an anisotropic QR ($\epsilon = 0.5$) and for different values of α_0 . Figure 3(a) displays the unusual AB oscillations without the ILF due to the structural anisotropy of the QR. With an increase in α_0 the effect of structural anisotropy on the energy levels weakens [Fig. 3(b)], and for $\alpha_0 = 3.2$ nm the usual AB oscillations are completely recovered [Fig. 3(c)]. A further increase in the ILF parameter

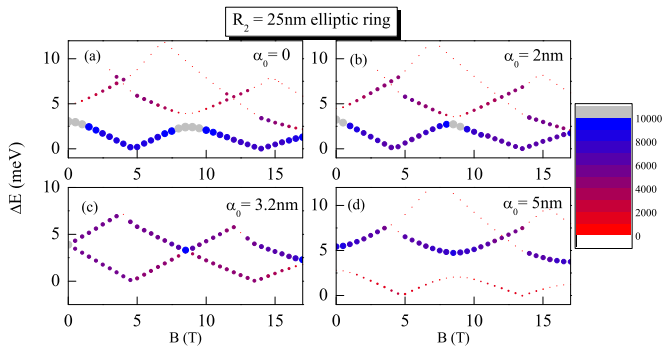


FIG. 6. Dipole-allowed optical transition energies as a function of the magnetic-field B for different values of the laser-field parameter α_0 . The results are for the $R_2 = 25$ -nm elliptic QR. The size and the color of the circles in the figure are proportional to the intensity of the calculated optical transitions.

again creates an anisotropy in the x direction, and again the unusual AB oscillations can be observed in Fig. 3(d). This behavior of the electronic states in a quantum ring is reported here. Similar effects also can be observed for smaller QRs, which are presented in Fig. 4. The influence of the ILF on the confinement potential of the QR is stronger for smaller QRs, and therefore the usual AB oscillations are recovered for $\alpha_0 = 2.1$ nm [see Fig. 4(c)].

These interesting properties of the energy spectra are expected to influence the optical properties of the QRs. In Fig. 5 the dipole-allowed optical transition energies as a function of the magnetic field are presented for different values of α_0 for isotropic QRs with outer radii of $R_2 = 25$ nm. The size and the color of the circles in this figure is proportional to the intensity $|M_{fi}|^2$ of the calculated optical transitions. Without the laser field the signature of the usual AB optical oscillations is seen in Fig. 5(a). The energies in Fig. 5(a) correspond to the transitions from the ground state to the first and second excited states. All other transitions are forbidden due to the cylindrical symmetry of the structure. With the increase in α_0 the unusual optical AB oscillations are again visible. Furthermore, it should be noted that with the increase in α_0 the intensity of the $1 \rightarrow 2$ transition weakens and the intensity of the $1 \rightarrow 3$ transition strengthens.

As an example, for $\alpha_0 = 5$ nm the $1 \rightarrow 2$ transition has almost disappeared. This fact can be explained by the anisotropy of the system created by the ILF in the x direction.

In Fig. 6 the same results as in Fig. 5 are presented for an anisotropic QR and for the value of $\varepsilon = 0.5$. Without the laser field the optical AB oscillations again have unusual behavior [Fig. 6(a)], but now the intensity of the $1 \rightarrow 2$ transition is stronger than that of $1 \rightarrow 3$. This is because the structural anisotropy is created in the y direction. With an increase in α_0 the intensity of $1 \rightarrow 3$ increases, and the intensity of $1 \rightarrow 2$ decreases. For the value of $\alpha_0 = 3.2$ nm the usual optical AB oscillations are completely recovered for an anisotropic QR [Fig. 6(c)]. Therefore we believe that these interesting effects can be confirmed experimentally.

In conclusion, we have studied here the strong influence of an intense terahertz laser field on the electronic and optical properties of isotropic and anisotropic QRs in an applied magnetic field. We have shown that in isotropic QRs the laser field creates the unusual AB oscillations, which are usually expected in anisotropic rings. Therefore with the laser field we can observe a continuous evolution of AB oscillations within the same ring. In the case of anisotropic QRs we have shown that with the ILF it is possible to completely control the anisotropy of the QR and thus the physical characteristics. In particular we have shown here that energy spectra and AB oscillations have been made completely usual by the ILF for anisotropic QRs. Lastly, it is worth noting that the ILF can in principle restore isotropic properties of a QR from any type of anisotropy (structural, effective masses, defects, etc.) of the QRs. We believe that, in addition to providing a unified picture of the electronic and optical properties of quantum rings, our studies will also open up new possibilities to design, fabricate, and improve new devices based on QRs, such as terahertz detectors, efficient solar cells, photon emitters, etc.

The work has been supported by the Canada Research Chairs Program of the Government of Canada, the Armenian State Committee of Science (Project No. 15T-1C331), CONICYT-ANILLO ACT Grant No. 1410, and the Center of Excellence with BASAL/CONICYT financing, Grant No. FB0807, CEDENNA.

- [1] Y. Aharonov and D. Bohm, *Phys. Rev.* **115**, 485 (1959).
- [2] M. Büttiker, Y. Imry, and R. Landauer, *Phys. Lett. A* **96**, 365 (1983).
- [3] A. Lorke, R. J. Luyken, A. O. Govorov, J. P. Kotthaus, J. M. Garcia, and P. M. Petroff, *Phys. Rev. Lett.* **84**, 2223 (2000).
- [4] U. F. Keyser, C. Fühner, S. Borck, R. J. Haug, M. Bichler, G. Abstreiter, and W. Wegscheider, *Phys. Rev. Lett.* **90**, 196601 (2003); A. Fuhrer, S. Lüscher T. Ihn, T. Heinzl, K. Ensslin, W. Wegscheider, and M. Bichler, *Nature (London)* **413**, 822 (2001).
- [5] T. Chakraborty, *Adv. Solid State Phys.* **43**, 79 (2003); S. Viefers, P. Koskinen, P. Singha Deo, and M. Manninen, *Physica E (Amsterdam)* **21**, 1 (2004); P. Pietiläinen and T. Chakraborty, *Solid State Commun.* **87**, 809 (1993); K. Niemelä, P. Pietiläinen, P. Hyvönen, and T. Chakraborty, *Europhys. Lett.* **36**, 533 (1996); T. Chakraborty and P. Pietiläinen, *Phys. Rev. B* **50**, 8460 (1994).
- [6] G. Huang, W. Guo, P. Bhattacharya, G. Ariyawansa, and A. G. U. Perera, *Appl. Phys. Lett.* **94**, 101115 (2009).
- [7] J. Wu, Z. M. Wang, V. G. Dorogan, S. Li, Z. Zhou, H. Li, J. Lee, E. S. Kim, Y. I. Mazur, and G. J. Salamo, *Appl. Phys. Lett.* **101**, 043904 (2012).
- [8] R. J. Young, E. P. Smakman, A. M. Sanchez, P. Hodgson, P. M. Koenraad, and M. Hayne, *Appl. Phys. Lett.* **100**, 082104 (2012).
- [9] R. J. Warburton, C. Schäfflein, D. Haft, F. Bickel, A. Lorke, K. Karrai, J. M. Garcia, W. Schoenfeld, and P. M. Petroff, *Nature (London)* **405**, 926 (2000).
- [10] M. Abbarchi, C. A. Mastrandrea, A. Vinattieri, S. Sanguinetti, T. Mano, T. Kuroda, N. Koguchi, K. Sakoda, and M. Gurioli, *Phys. Rev. B* **79**, 085308 (2009).
- [11] D. S. L. Abergel, V. Apalkov, J. Berashevich, K. Ziegler, and T. Chakraborty, *Adv. Phys.* **59**, 261 (2010); *Physics of Graphene*,

- edited by H. Aoki and M. S. Dresselhaus (Springer, New York, 2014); J. Berashevich and T. Chakraborty, *Nanotechnology* **21**, 355201 (2010).
- [12] A. Tsukazaki, A. Ohtomo, T. Kita, Y. Ohno, H. Ohno, and M. Kawasaki, *Science* **315**, 1388 (2007); A. Tsukazaki, S. Akasaka, K. Nakahara, Y. Ohno, H. Ohno, D. Maryenko, A. Ohtomo, and M. Kawasaki, *Nature Mater.* **9**, 889 (2010); J. Falson, D. Maryenko, B. Friess, D. Zhang, Y. Kozuka, A. Tsukazaki, J. H. Smet, and M. Kawasaki, *Nat. Phys.* **11**, 347 (2015).
- [13] D. S. L. Abergel, V. M. Apalkov, and T. Chakraborty, *Phys. Rev. B* **78**, 193405 (2008); M. Zarenia, B. Partoens, T. Chakraborty, and F. M. Peeters, *ibid.* **88**, 245432 (2013).
- [14] T. Chakraborty, A. Manaselyan, and M. Barseghyan, *J. Phys.: Condens. Matter* **29**, 215301 (2017).
- [15] *Physics of Quantum Rings*, edited by V. M. Fomin (Springer-Verlag, Berlin/Heidelberg, 2014).
- [16] R. Blossey and A. Lorke, *Phys. Rev. E* **65**, 021603 (2002).
- [17] P. Offermans, P. M. Koenraad, J. H. Wolter, D. Granados, J. M. Garcia, V. M. Fomin, V. N. Gladilin, and J. T. Devreese, *Appl. Phys. Lett.* **87**, 131902 (2005).
- [18] N. A. J. M. Kleemans, I. M. A. Bominaar-Silkens, V. M. Fomin, V. N. Gladilin, D. Granados, A. G. Taboada, J. M. Garcia, P. Offermans, U. Zeitler, P. C. M. Christianen, J. C. Maan, J. T. Devreese, and P. M. Koenraad, *Phys. Rev. Lett.* **99**, 146808 (2007).
- [19] J. Wu, Z. M. Wang, K. Holmes, E. Marega, Jr., Z. Zhou, H. Li, Y. I. Mazur, and G. J. Salamo, *Appl. Phys. Lett.* **100**, 203117 (2012).
- [20] T. Raz, D. Ritter, and G. Bahir, *Appl. Phys. Lett.* **82**, 1706 (2003).
- [21] J. Sormunen, J. Riikonen, M. Mattila, J. Tiilikainen, M. Sopanen, and H. Lipsanen, *Nano Lett.* **5**, 1541 (2005).
- [22] V. M. Fomin, V. N. Gladilin, S. N. Klimin, J. T. Devreese, N. A. J. M. Kleemans, and P. M. Koenraad, *Phys. Rev. B* **76**, 235320 (2007).
- [23] J. Planeles, F. Rajadell, and J. I. Climente, *Nanotechnology* **18**, 375402 (2007).
- [24] G. A. Farias, M. H. Degani, J. A. K. Freire, J. Costa e Silva, and R. Ferreira, *Phys. Rev. B* **77**, 085316 (2008).
- [25] L. Wendler, V. M. Fomin, and A. A. Krokhin, *Phys. Rev. B* **50**, 4642 (1994).
- [26] L. Wendler and V. M. Fomin, *Phys. Status Solidi B* **191**, 409 (1995).
- [27] M. M. Milošević, M. Tadić, and F. M. Peeters, *Nanotechnology* **19**, 455401 (2008).
- [28] A. Ghazaryan, A. Manaselyan, and T. Chakraborty, *Phys. Rev. B* **93**, 245108 (2016).
- [29] G. O. de Sousa, D. R. da Costa, A. Chaves, G. A. Farias, and F. M. Peeters, *Phys. Rev. B* **95**, 205414 (2017).
- [30] W. C. Henneberger, *Phys. Rev. Lett.* **21**, 838 (1968).
- [31] M. Gavrilu and J. Z. Kaminski, *Phys. Rev. Lett.* **52**, 613 (1984).
- [32] M. Pont, N. R. Walet, M. Gavrilu, and C. W. McCurdy, *Phys. Rev. Lett.* **61**, 939 (1988).
- [33] E. C. Valadares, *Phys. Rev. B* **41**, 1282(R) (1990).
- [34] M. Gavrilu, *J. Phys. B* **35**, R147 (2002).
- [35] *Intense Terahertz Excitation of Semiconductors. Semiconductor Science and Technology*, edited by S. D. Ganichev and W. Prettl (Oxford University Press, Oxford, 2006).
- [36] M. Bukov, L. D'Alessio, and A. Polkovnikov, *Adv. Phys.* **64**, 139 (2015).
- [37] M. Gavrilu, *Atoms in Intense Laser Fields* (Academic, New York, 1992).
- [38] H. M. Baghrmian, M. G. Barseghyan, and D. Laroze, *Sci. Rep.* **7**, 10485 (2017).
- [39] See Supplemental Material at <http://link.aps.org/supplemental/10.1103/PhysRevB.97.041304> for a complete derivation of Eq. (3) from Eq. (1).
- [40] A. Radu, A. A. Kirakosyan, D. Laroze, H. M. Baghrmian, and M. G. Barseghyan, *J. Appl. Phys.* **116**, 093101 (2014).
- [41] A. Radu, A. A. Kirakosyan, D. Laroze, and M. G. Barseghyan, *Semicond. Sci. Technol.* **30**, 045006 (2015).
- [42] S. Adachi, *Handbook on Physical Properties of Semiconductors* (Kluwer Academic, New York, 2004), Vol. 2.